Part II

Experimental Methods

3 Probing the Nodal Structure

The topology and k-spatial symmetry of zeroes of the gap function provide useful information on the superconductive order parameter. Besides direct, i. e. spectroscopic probes of the nodal structure, bulk methods are usually used as an integral probe of the low-energetic excitation spectrum at low temperature. In the following sections frequently applied methods are discussed.

3.1 Specific Heat and Thermal Conductivity

The determination of the heat capacity of a substance provides information about its internal energy. Specific heat is a bulk method which probes at low temperature the entire low-energy excitations of a solid close to the Fermi level, i. e., it is sensitive to the density of states at E_F. The thermal conductivity is a transport property and a directional probe, which depends on the direction of the applied thermal gradient. Therefore, the thermal conductivity is capable to reveal the orientation and symmetry of nodes in the gap function. Thermal-conductivity measurements on metals are sensitive to the density of states at E_F, as for metals at low temperatures primarily electrons near the Fermi surface are responsible for the transport of energy.

In a standard s-wave superconductor with opening of an isotropic excitation gap at the Fermi surface below T_c the specific heat $C(T)$ and the thermal conductivity $\kappa(T)$ vanish exponentially in the limit $T \to 0$. The existence of line or point nodes alters this behaviour. The existence of quasiparticle excitations in the neighbourhood of these nodes gives rise to a non-exponential behaviour of both quantities, particularly at low temperatures where the node contributions are dominant. These low-energetic excitations are responsible for power laws $\sim T^n$ in the temperature dependence of both properties for $T \to 0$ and the exponent n of T hints at the nodal structure of the order parameter. For example, a T^2 behaviour of the specific heat at $T \ll T_c$ hints at line nodes, while $C(T) \sim T^3$ indicates point nodes of the gap function. A list of exponents n of the low-temperature behaviour of $C(T)$ calculated under the aspect of order-parameter symmetry was published by Volovik and Gor'kov [1].

However, the hint at the nodal structure might be hidden by extrinsic origins of low-lying states within Δ. In particular, impurities are at the forefront of the extrinsic origins. On the other hand, if the impurity concentration is sufficiently low, the dependence of the transport properties on the impurity concentration itself makes

G. Goll: *Unconventional Superconductors*
STMP **214**, 21–26 (2006)

it feasible to uncover information on the order-parameter symmetry. It has been shown [2, 3] that the effect of impurity scattering on the transport properties can only be addressed if the scattering is in the strong scattering (unitary) limit, i. e. a phase shift of $\delta_0 = \pi/2$ is involved in the scattering process. In this case, the temperature dependence of the thermodynamic properties is quantitatively related to the density of states and shows power laws depending on the position and form of the line or point nodes of the superconducting gap. If the scattering phase shift is near the Born limit $\delta = 0$ no clear predictions can be made.

Unitary scattering leads to virtual bound states on the impurity sites. For the typical concentration of impurities, these bound states overlap and lead to a small "normal state-like" contribution (linear in T) to κ. Theoretically, it can be described by the development of a new energy scale γ, below which the density of states is nearly constant and in particular, finite at the Fermi level. The parameter γ is interpreted as the bandwidth of quasiparticle states bound to impurities [4] and provides a crossover energy scale as well. For energies larger than γ the transport properties of unconventional superconductors are determined by the quasiparticle excitations at the nodes, below γ the transport properties are dominated by the bound states. The energy scale and the zero-energy density of states depend on both the impurity concentration and the scattering phase shift δ_0. Graf et al. [5, 6] calculated the electronic contribution to the thermal conductivity for various order-parameter symmetries and found for some a *universal* value as the temperature approaches zero. *Universal* means that the thermal conductivity becomes independent of the impurity concentration and $\kappa/T = const$ (see Fig. 3.1). Thus, experiments on unconventional superconductors with controlled impurity concentrations might allow to distinguish various order-parameter scenarios, depending on whether or not they approach a universal limit.

A second test for the order-parameter symmetry arises from the magnetic-field dependence of thermal conductivity and specific heat. As pointed out by Volovik [7] the density of states in a magnetic field in superconductors with order-parameter nodes is dominated by contributions from extended quasiparticle states rather than the bound states associated with the vortex cores. The remarkable consequence of this observation is a term in the specific heat varying as $\sqrt{HT}$ for a line node. Kübert and Hirschfeld [8] derived a scaling law for the quasiparticle transport properties in the variables $T/\sqrt{H}$, mixing field and temperature dependence, which can be used as a test of the nodal structure, as no scaling is expected, e. g. for linear point nodes.

A third experimental tool for probing the superconducting gap structure has been established recently by Izawa and coworkers [9]. They used angular-dependent thermal conductivity in the vortex state to study nodal superconductors. The most remarkable effect for the understanding of the heat transport in the mixed state is the Doppler shift of the delocalized quasiparticle spectrum which is generated by the supercurrents around the vortices. This effect gives rise to the finite density of states in the presence of nodes, at which the Doppler shift exceeds the local energy gap [10, 11, 12, 13].

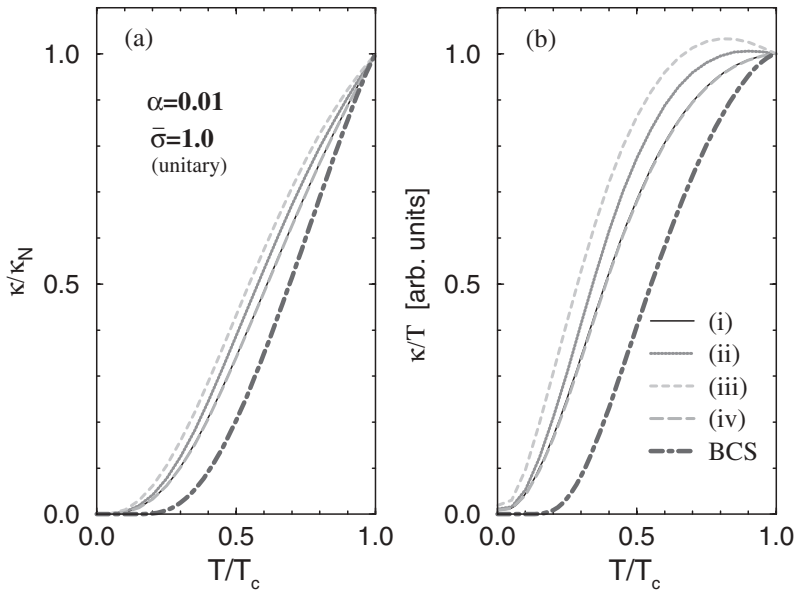

Fig. 3.1. Thermal conductivity κ vs. temperature for unconventional superconductors in the unitary limit ($\overline{\sigma} = 1$) with a dimensionless scattering rate $\alpha = 0.01$. The different pairing states are: (i) $d_{x^2-y^2}$ with $B_{1g}(D_{4h})$ symmetry and 4 linear line nodes, (ii) polar state with $A_{1u}(D_{6h})$ symmetry and 1 linear line node, (iii) hybrid I state with $E_{1g}(D_{6h})$ symmetry and 2 linear point nodes and 1 linear line node, and (iv) hybrid II state with $E_{2u}(D_{6h})$ symmetry and 2 quadratic point nodes and 1 linear line node. For comparison the result for an isotropic BCS superconductor is shown (by courtesy of M. Graf, LANL). As pointed out by Graf and coworkers κ/T has a finite intercept for the unconventional pairing states (i) – (iv)

3.2 Magnetic Penetration Depth

A further probe for the nodal structure are measurements of the magnetic penetration depth λ. Two methods have been established to give access to this quantity, namely measurements of the surface impedance in a microwave resonator and transverse-field μSR studies. The measurements of the surface impedance Z_s have played a key role in expanding the understanding of superconductivity. Microwave measurements are made in cavity resonators applying resonance modes with frequencies f_0 in the GHz range. Such measurements probe the complex conductivity $\sigma = \sigma' - i\sigma''$ as a function of temperature and frequency, from which the superfluid density as well as the properties of the thermally excited quasiparticles can be deduced. The surface resistance and changes in surface reactance of the sample mounted inside the resonator are obtained from the full-width at half-maximum and the changes of f_0 of the resonance curves. In the local limit of the two-fluid model [14] the surface impedance and complex conductivity are given by

$$Z_s = R_s + iX_s = \left(\frac{i\mu_0\omega}{\sigma' - i\sigma''}\right)^{1/2} , \tag{3.1}$$

where the real part R_s is the surface resistance and the imaginary part X_s is the surface reactance. The two-fluid model gives a conductivity

$$\sigma = \left(\frac{e^2}{m^*}\right)\left[\frac{n_s}{i\omega} + \frac{n_n\tau}{1 + i\omega\tau}\right], \tag{3.2}$$

where $n_s = 1 - n_n$ is the superfluid density, and n_n is the normal fluid density; in the superconducting state, τ is the scattering lifetime of the thermally excited quasiparticles and m^* is their effective mass. Both contributions to the surface impedance and complex conductivity reflect that in the two-fluid model most of the current at frequencies in the microwave range will be carried as a lossless supercurrent, but there will be dissipation from the normal component for any nonzero frequency. The magnetic penetration depth λ and its temperature dependence is obtained from $n_s = \lambda(0)^2/\lambda(T)^2$ which is derived from σ''.

The second possibility for the determination of the magnetic penetration depth are transverse-field μSR studies (see Sect. 4.3). In type-II superconductors the presence of the flux-line lattice causes an additional line broadening of the μSR line which is assumed to be Gaussian. The muon depolarization rate then is given by $1/\lambda^2 \propto n_s$, where λ is the magnetic penetration depth and n_s the superfluid density.

Such studies yield information on the absolute value of λ, its anisotropy, and the temperature dependence $\lambda(T)$ which is altered in the presence of gap nodes. However, one has to be cautious against such experiments. As already pointed out by Tinkham [14] the magnetic penetration depth λ^{-2} cannot have a universal temperature dependence on T/T_c even in the BCS theory because of the variation of the ratio $\xi_0/\lambda_L(0)$ for different metals. The temperature dependence slightly differs in the *pure local limit* ($l \gg \xi, \xi \ll \lambda$), the *pure anomalous limit* ($l \gg \xi, \xi \gg \lambda$), and the *dirty local limit* ($l \ll \xi, \xi \ll \lambda$) compared to the empirical approximation of the two-fluid model given by

$$\frac{\lambda(T)}{\lambda(0)} = \frac{1}{[1 - (T/T_c)^4]^{1/2}} \tag{3.3}$$

i. e. an exponent $n = 4$ for $\lambda^{-2} \propto 1 - (T/T_c)^n$. In a clean, local, weak-coupling BCS superconductor the exponent n is generally closer to $n = 2$ than to $n = 4$ [14]. For d-wave order parameter the temperature dependence is altered as well. The presence of line nodes gives rise to a continuum of low-lying excitations which results in a linear temperature dependence of $\lambda^{-2} \propto n_s$. Further, according to calculations by Hirschfeld and Goldenfeld [15] the presence of impurities leads to a crossover to a quadratic temperature dependence at low T.

3.3 Ultrasound Attenuation

The last method which is introduced here is the use of ultrasound-attenuation measurements, a rarely utilized tool for probing the gap nodes. When a sound wave propagates through a metal the microscopic electric field due to the displacement of

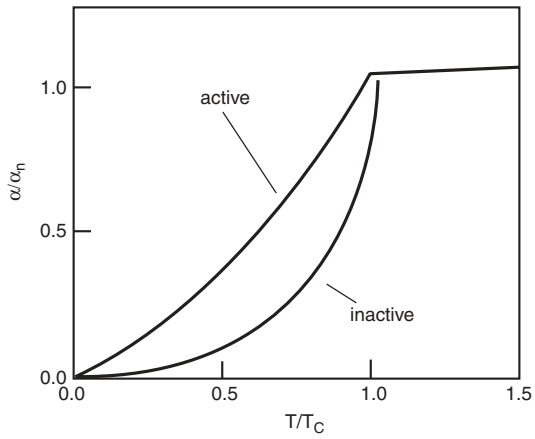

Fig. 3.2. Qualitative behavior of the ultrasound attenuation in the superconducting state. In the presence of "active" nodes the attenuation grows by a factor T^2 faster than in the presence of "inactive" nodes at low T (from [17])

the ions can impart energy to electrons near the Fermi level, thereby removing energy from the wave. In a superconductor well below T_c the rate of attenuation $\alpha(T)$ of sound waves with $\hbar\omega < 2\Delta$ is markedly lower than in a normal metal. Therefore, measurements of the ultrasonic attenuation allow the determination of the temperature dependence and the anisotropy of the energy gap. Moreno and Coleman have developed a simple theory for the interpretation of transverse ultrasound attenuation coefficients in systems with nodal gap anisotropy [16]. In their calculations, performed in the hydrodynamic limit where the electron mean free path ℓ is much shorter than the sound wavelength λ, the low temperature power-law behaviour of $\alpha(T)$ is shown to depend strongly on the wave-vector direction $\hat{q}$ and the polarization $\hat{e}$ relative to the nodes. Nodes are "active" in attenuating sound, if neither of these vectors is perpendicular to the direction of the node, while nodes are "inactive" if either the vector $\hat{q}$ or the polarization $\hat{e}$ are perpendicular to the direction of the node. In this way ultrasound-attenuation experiments can locate nodes in the gap function. Based on the idea of "active" and "inactive" nodes Walker et al. worked out a more generalized theory by replacing the isotropic electron stress tensor in [16] by the electron-phonon matrix element. They derived an expression which is also applicable to anisotropic multisheet Fermi surfaces. If the matrix element is non-zero at the nodes for a particular phonon then the phonon can interact with the nodal quasiparticle (and thus attenuate a sound wave), i. e. the node is "active" for the particular phonon. If, on the other hand, the matrix element is zero at the nodes, then the coupling of the phonon to the quasiparticle precisely at the node is zero and grows as the distance from the node is increased. In this case, the node is "inactive" for the particular phonon [17].

In addition to the interpretation of ultrasound attenuation data, Moreno and Coleman have predicted a $T^{3.5}$ power law for the direction of inactive nodes and

a $T^{1.5}$ power law for the direction of active nodes for the case of a two-dimensional gap with $k_x^2 - k_y^2$ symmetry. In general, the ultrasound attenuation at $T \ll T_c$ exhibits a power law behaviour and the exponent n is larger by two in the case where only "inactive" nodes are present compared to the case when "active" nodes are present (see Fig. 3.2).

References

1. G.E. Volovik, L.P. Gor'kov: Sov. Phys. JETP **61**(4), 843 (1985). (Zh. Eksp. Teor. Fiz. **88**, 1412 (1985)) 11, 14, 17, 21
2. P. Hirschfeld, D. Vollhardt, P. Wölfle: Solid State Commun. **59**(3), 111 (1986) 22, 50, 98
3. P.J. Hirschfeld, P. Wölfle, D. Einzel: Phys. Rev. B **37**, 83 (1988) 22, 50
4. L.J. Buchholtz, G. Zwicknagl: Phys. Rev. B **23**(11), 5788 (1981) 22, 36
5. M.J. Graf, S.K. Yip, J.A. Sauls: J. Low Temp. Phys. **102**, 367 (1996) 22, 74, 75, 91, 92, 93, 125
6. M.J. Graf, S.K. Yip, J.A. Sauls, D. Rainer: Phys. Rev. B **53**(22), 15 147 (1996) 22
7. G.E. Volovik: JETP Lett. **58**(6), 469 (1993). (Pis'ma Zh. Eksp. Teor. Fiz. **58**, 457 (1993)) 22
8. C. Kübert, P.J. Hirschfeld: Phys. Rev. Lett. **80**(22), 4963 (1998) 22
9. K. Izawa, Y. Matsuda: J. Low Temp. Phys. **131**(3/4), 429 (2003) 22
10. P. Thalmeier, K. Maki: Europhys. Lett. **58**(1), 119 (2002) 22
11. I. Vekhter, P.J. Hirschfeld, J.P. Carbotte, E.J. Nicol: Phys. Rev. B **59**(14), R9023 (1999) 22, 124
12. K. Maki, G. Yang, H. Won: Physica C **341-348**(3), 1647 (2000) 22
13. H. Won, K. Maki: cond-mat/0004105 (2000) 22, 124
14. M. Tinkham: *Introduction to Superconductivity* (McGraw-Hill International Editions, Singapore, 1996) 11, 23, 24, 29, 56
15. P.J. Hirschfeld, N. Goldenfeld: Phys. Rev. B **48**(6), 4219 (1993) 24, 75, 125
16. J. Moreno, P. Coleman: Phys. Rev. B **53**(6), R2995 (1996) 25
17. M.B. Walker, M.F. Smith, K.V. Samokhin: Phys. Rev. B **65**, 014 517 (2002) 25, 95